

High-Temperature Stability of Passivated Silver Nanocrystal Superlattices

S. A. Harfenist

School of Physics, Georgia Institute of Technology, Atlanta, Georgia 30332-0430

Z. L. Wang*

School of Materials Science and Engineering, Georgia Institute of Technology, Atlanta, Georgia 30332-0245

Received: January 4, 1999; In Final Form: February 25, 1999

Ordered arrays of ~ 4.5 nm diameter silver nanocrystals passivated with dodecanethiol show remarkable thermal stability at temperatures up to 975 K. Defects in the ordered-assembly were the first areas to show signs of melting while much of the structure remained intact. The mechanism for their stability is attributed to the unusually strong inter-nanocrystal bond formed by the interpenetration of thiol chains between neighboring nanocrystals within the nanocrystal superlattice. Individually dispersed nanocrystals show stability up to 800 K while some persist until 975 K.

The potential application of nanoscale materials in fields ranging from biology to electronics has spurred remarkable interest and investigation into the preparation and characterization of identical, isolated, nanometer-scale entities composed of materials such as metals,^{1,2} semiconductors,³ magnetic materials,⁴ and a wide variety of others.^{5,6} Applications in catalysis and biological tagging⁷ and the possibility of nanometer-sized magnetic domains for ultrahigh-density recording media⁴ are just a few of their many possible uses. The subsequent organization of identical passivated nanometer-scale objects into micron-scale ordered arrays gives encouragement to the use of these novel materials particularly in regards to their collective nonlinear optical properties where stability at high temperatures is necessary.⁸

The studies of nanometer-sized crystallites over the past twenty years and more recently their composite structures have been numerous.^{9,10} Various methods are being used to produce these materials in such abundance as to allow their characterization by means of well-known chemical and physical techniques.^{6,11,12} The solution phase, gas (aerosol) phase, and reverse-micelle methods have been the most popular nanocrystal production techniques lately.

An important factor in the production of nanocrystals is the ability to keep them physically isolated from one another. Many different types of systems have been used for nanocrystal passivation as well as exchange of one surfactant for another.^{3,7,13} Factors such as the binding energy of the headgroups to the nanocrystal surface,¹⁴ how the exposed tails affect the solubility and reactivity of the passivated nanocrystal (i.e., its functionality),¹⁰ the effect of the passivation agent on the electronic and optical properties of the nanocrystal core, the electronic properties of the surfactant material itself,¹⁵ and, further, the agent's ability to bind or link nanocrystals together both structurally and electronically^{16–18} are all very important conditions placed on a material that will allow the nanocrystal to be stable and isolated yet not affect its core material's properties. Here we present an in-situ temperature analysis of

the aforementioned nanocrystals and their superlattices and show that not only do individual passivated silver nanocrystals supported on an amorphous carbon film remain stable at temperatures near 800 K, but also that the silver nanocrystal supercrystals (Ag NCSs) show structural stability near 975 K.

Previous work determined the structure and properties of NCSs composed of ca. 4.5 nm core diameter silver nanocrystals passivated with dodecanethiol (SC₁₂H₂₅) self-assembled-monolayers (SAMs), having an approximate length of 1.2 nm projecting from the nanocrystal surface.² The silver nanocrystals were produced using an aerosol method described elsewhere.² The icosahedral (20-faceted) silver nanocrystals show even longer micron-range ordering of their subsequent superlattice than similar mass truncated octahedral nanocrystals¹⁸ and, further, exhibit a similar type of weblike nanocrystal interconnects throughout their hexagonal-close-packed superlattice. The NCSs measure ~ 0.2 – 3.0 μm laterally and have very uniform, platelet-like structure in thickness, here ~ 15 nanocrystal layers thick (Figure 1). The TEM micrographs obtained clearly show the long-range order and faceting of the resulting supercrystals. The corrugations seen in the inset of Figure 1 are the lattice planes of silver nanocrystals viewed along the [0001] zone axis. Away from the dark contrast of the supercrystals one can see individual nanocrystal resolution as dark dots scattered over the film.

A Gatan TEM specimen heating stage was employed to carry out the in-situ experiment in a Hitachi HF2000 Field Emission Gun Transmission Electron Microscope. The specimen temperature could be increased continuously from room temperature to 975 K. The heating unit is made of a Ta cup on which the specimen is loaded. The column pressure was kept at 2×10^{-8} Torr. The temperature was increased from room temperature at a rate of approximately 3 K/min.

Shown in Figure 2a–d are subsequent images of the same region of a NCS at temperatures of 600 K (a), 740 K (b), 820 K (c) and 975 K (d). The region seen consists of two supercrystals that overlap (darker contrast) near the upper left of the images. In Figure 2a, one can easily make out the nanocrystal packing structure of each supercrystal domain. As evident by the figure, they remain almost perfectly intact up to

* Author to whom all correspondence should be addressed. E-mail: zhong.wang@mse.gatech.edu.



Figure 1. Transmission Electron Micrograph of silver nanocrystal superlattices composed of ~ 4.5 nm diameter Ag cores passivated with dodecanethiol self-assembled-monolayers (SAMs). The ordered hexagonal-close-packed structure can be seen in the inset, a high magnification of the boxed region in Figure 1. Apparent in the inset are the corrugations corresponding to nanocrystal lattice planes in the supercrystals and individually dispersed nanocrystals on the carbon film between the supercrystals.

820 K (Figure 2c). Remarkably, at 975 K (Figure 2d) much of the supercrystal structure still remains unaltered. Of interest are the areas marked A and B in Figure 2a–d. These are defects in the packing structure of the superlattices, and careful observation of these regions shows that as the temperature is increased these become increasingly larger regions of melting and coagulation of the nanocrystal cores while the rest of the supercrystal remains intact. It is apparent from the micrographs that the edges of the supercrystals remain stable while toward the center superlattice contrast becomes obscure as potentially the upper layers of nanocrystals in the superlattice have lost their protective mantle of surfactant and melted, pulling back from the NCS edges, while the lower layers have not. Of further interest are the images of individual nanocrystals seen on the carbon film separate from the NCSs (indicated by arrowheads in Figure 2a).

If one looks at subsequently higher temperatures it is seen that the dispersed individual nanocrystals stay intact on the carbon film well up to 740 K (Figure 2b). Thereafter, an apparent loss of most of these particles by 975 K either due to evaporation or motion laterally along the carbon film takes place.

An understanding of how the passivating self-assembled-monolayers (SAMs) protect the nanocrystal surface and, more importantly, facilitate the obviously very strong inter-nanocrystal bonding can be developed from work done on SAMs passivating atomically flat gold, silver, and copper surfaces.^{19–23} The bonding of the thiols to the metal surfaces is mediated by the sulfur–surface bond. Various length thiol chains, ranging from propanethiol (C3) to octadecanethiol (C18), have been shown to cover these noble metal surfaces, effectively rendering them inert to oxidation or contamination. Alkylthiol coverage of gold

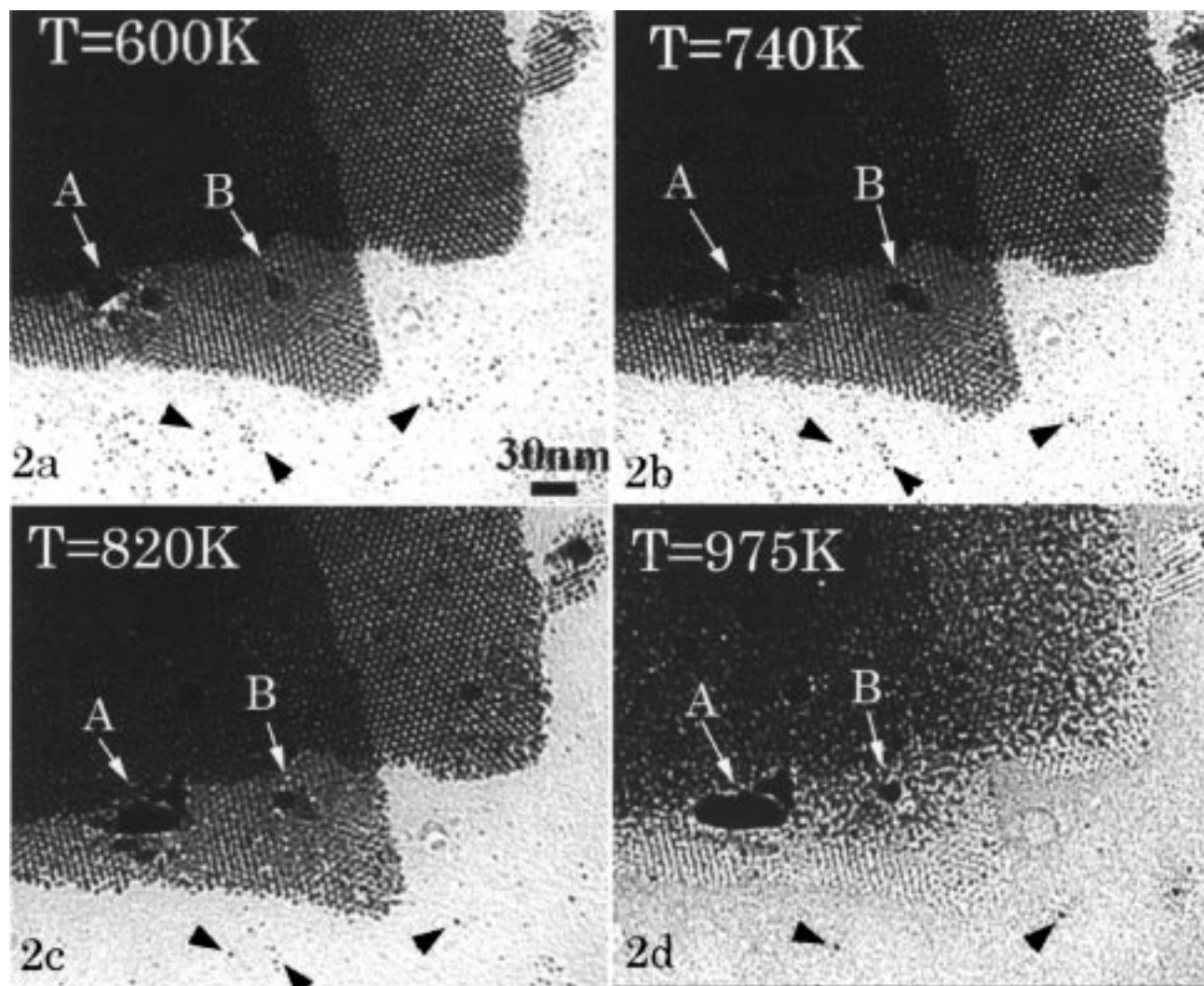


Figure 2. Transmission electron micrograph images of a silver nanocrystal supercrystal recorded in-situ at (a) $T = 600$ K, (b) $T = 740$ K, (c) $T = 820$ K, and (d) $T = 975$ K. The specimen was held at each temperature for ~ 10 min for data recording. Areas marked A and B correspond to defects in the superlattice (Figure 2a) that show increasing contrast with temperature owing to coagulation of melted silver nanocrystal cores. Individually dispersed nanocrystals (arrowheads) show stability through 740 K (Figure 2b) and even up to 975 K.

and silver surfaces, usually the $\{111\}$ and $\{110\}$ surfaces, have been well studied. Calculations show that the sulfur–surface distance is longer for silver than for the same indexed gold surface.¹⁴ Structurally, the degree of tilt of the carbon backbone of the molecules from the surface normal was found to have a tilt of approximately 30° for gold, while for silver a smaller angle ranging from ~ 0 – 17° ,^{22,24} was found, indeed, some further conclude that the angle of tilt for thiols on silver is closer to 0° .¹⁴ This property of near-normal projection of the thiol molecules from silver surfaces would allow greater interdigitation among thiols on neighboring nanocrystals and gives some insight into, generally, why we have seen that superlattices of thiol-passivated Ag nanocrystals might show better long-range ordering than similar superlattices comprised of Au nanocrystals.

Much of the present understanding of SAM formation and structure on noble metal surfaces has been from experimentation on gold surfaces. Since Au and Ag share many common properties, especially concerning their passivation with SAMs, it seems only natural to discuss data from SAM experiments utilizing gold to support this work done on silver. Also, much of the data gained about thiol interdigitation between gold nanocrystals, presumably, has very little dependence upon the surface they are coating.

Thiol-covered gold surfaces show thermal desorption complete by 500 K, but desorption started at slightly lower temperatures, 425–450 K, for silver.²⁰ Molecular dynamic calculations on < 2 nm core diameter gold nanocrystals show that the thiols have an ordering particular to the facet of the nanocrystal from which they project. The thiol chains tend to group together forming “bundles” of molecules projecting from the surface, allowing the nanocrystals to pack into a superlattice by interlocking their bundled thiol chains.²⁴ Experimental work on gold nanocrystals of ~ 1.2 nm diameter show that they pack together with thiols on neighboring nanocrystals interdigitating and forming a seemingly organized molecular bond between the nanocrystal cores. The amount of interpenetration is roughly proportional to the thiol chain length (here C8, 12, and 16) and the inter-nanocrystal spacing quite less than twice the thiol chain length.²⁶ This is concurrent with thiol chain interdigitation and agrees with our previously measured inter-nanocrystal spacings for silver NCSs.^{2,18}

Direct imaging and simultaneous chemical composition analysis of Ag nanocrystal interconnects within a NCS was achieved using energy-filtering TEM.¹⁷ This proves that the thiol molecules used to passivate the nanocrystal core surfaces are directly connecting facets of neighboring nanocrystals. The thiol

density is highest along the line of nearest neighbor nanocrystal cores and lowest in the interstitial regions agreeing with image contrast seen in previous work.¹⁸ The Ag nanocrystals show bundling of the passivating thiols with interdigitation of thiol chain bundles, not interlocking of the bundles, like gears, that would fill the space between the cores uniformly.^{17,18}

From Figure 2 one can see through this experiment that when packed into a supercrystal the dodecanethiol molecules and nanocrystal silver cores are more stable. For continued observation of superlattice imaging up to 975 K the nanocrystal cores must remain isolated and the inter-nanocrystal bonding must persist or the cores would all coalesce, becoming areas of (molten) silver after evaporation of the passivating thiols from the core's surface (Figure 2 see A and B) and/or loss of inter-nanocrystal bonding between the thiol tail-groups. For the passivation of the nanocrystal cores to continue the thiol tail-groups must be structurally stabilized since their melting starts at the tail-groups and continues in toward the nanocrystal core.²⁵ The work done on extended 2D surfaces passivated with alkylthiol SAMs gives us reason to believe that thiols on flat surfaces (with tail-groups that are not bundled or bound together) are structurally less stable (desorb by ~500 K). Measurement of the thermal properties of SAMs on flat extended Ag surfaces show complete desorption by 500 K for hexadecane and octadecanethiols, starting around 450–475 K.^{19,20} It is proposed that this thiol stability on nanocrystalline silver at elevated temperatures could be attributed to the thiol tail-groups being bound in place. For both the thiol passivant and metal nanocrystal core to remain intact at temperatures in excess of twice that experimentally found for thiol molecules to desorb from flat surfaces, one must conclude that the bonding of the metal nanocrystals accomplished through the thiol passivation is much stronger than ever thought before and must occur in such a way as to keep the thiol tail-groups bound in place. The most obvious mechanism for these observations is the interdigitation of the bundled thiol tail-groups between neighboring nanocrystal cores.

Interaction of the NCS with the substrate is an important factor. As noted above, while the edges of the NCS stay intact, imaging of the center becomes obscure. This could be due to layers of the superlattice closer to the substrate being more stable while those near the top surfaces of the crystal melt and coagulate, pulling away from the edges (Figure 2a–d). This may be the reason that individual nanocrystals are still seen at these elevated temperatures, they are adhered to the substrate. Other reasons for apparent individual nanoparticle stability could be that the thiols have evaporated off the nanocrystal core and that the molten nanocrystal core of silver beads on the carbon surface, but the wetting of silver on amorphous carbon is not completely understood.

In summary, silver nanocrystals of ~4.5 nm core diameter, passivated with dodecanethiol SAMs, that pack into periodic NCSs, show remarkable stability at temperatures in great excess

of that needed to evaporate dodecanethiol from flat noble metal surfaces and melt nanocrystalline silver. The stability of the supercrystals is attributed to the unusually strong inter-nanocrystal bonding in the superlattice facilitated by the interdigitation of neighboring nanocrystals' dodecanethiol surfactant chains. Defects in the superlattice lead to areas of coalescence of molten silver, emphasizing the strength and stability of the thiol molecules when interdigitating with other bundled thiol molecules from neighboring nanocrystals.

Acknowledgment. Thanks to Dr. I. Vezmar and Dr. M. M. Alvarez for providing the specimen and stimulating discussion. We gratefully acknowledge the support of NSF DMR-9733160 and the Georgia Tech Molecular Design Institute, under prime contract N00014-95-1-1116 from the Office of Naval Research.

References and Notes

- (1) Cleveland, C. L.; Landman, U.; Shafiqullin, M. N.; Stephens, P. W.; Whetten, R. L. *Z. Phys. D* **1997**, *40*, 503.
- (2) Harfenist, S. A.; Wang, Z. L.; Alvarez, M. M.; Vezmar, I.; Whetten, R. L. *Adv. Mater.* **1997**, *9*, 817.
- (3) Alivisatos, A. P. *Science* **1996**, *271*, 933.
- (4) Yin, J. S.; Wang, Z. L. *Phys. Rev. Lett.* **1997**, *79*, 2570.
- (5) Prozorov, T.; Gedanken, A. *Adv. Mater.* **1998**, *10*, 532.
- (6) Motte, L.; Pileni, M. P. *J. Phys. Chem. B* **1998**, *102*, 4104.
- (7) Hainfeld, J. F.; Furuya, F. R. *J. Histochem. Cytochem.* **1992**, *40*, 177.
- (8) Collier, C. P.; Saykally, R. J.; Schiang, J. J.; Henrichs, S. E.; Heath, J. R. *Science* **1997**, *277*, 1978.
- (9) Marks, L. D. *Rep. Prog. Phys.* **1994**, *57*, 603.
- (10) Antonietti, M.; Goltner, C. *Angew. Chem., Int. Ed. Engl.* **1997**, *36*, 910.
- (11) Brust, M.; Fink, J.; Bethell, D.; Schiffrin, D. J.; Kiely, C. J. *Chem. Soc., Chem. Commun.* **1995**, 1655.
- (12) Vezmar, I. Ph.D. Dissertation, Georgia Institute of Technology, Atlanta, GA, 1998.
- (13) Andres, R. P.; Bielefeld, J. D.; Henderson, J. I.; Janes, D. B.; Kolagunta, V. R.; Kubiak, C. P.; Mahoney, W. J.; Osifchin, R. G. *Science* **1996**, *273*, 1690.
- (14) Sellers, H.; Ulman, A.; Shnidman, Y.; Eilers, J. E. *J. Am. Chem. Soc.* **1993**, *115*, 9389.
- (15) Samanta, M. P.; Tian, W.; Datta, S.; Henderson, J. I.; Kubiak, C. P. *Phys. Rev. B* **1996**, *53*, R7626.
- (16) Brust, M.; Bethell, D.; Schiffrin, D. J.; Kiely, C. J. *Adv. Mater.* **1995**, *7*, 795.
- (17) Wang, Z. L.; Harfenist, S. A.; Whetten, R. L.; Bentley, J.; Evans, N. D. *J. Phys. Chem. B* **1998**, *102*, 3068.
- (18) Harfenist, S. A.; Wang, Z. L.; Alvarez, M. M.; Vezmar, I.; Whetten, R. L. *J. Phys. Chem. B* **1996**, *100*, 13904.
- (19) Heinz, B.; Morgner, H. *Surf. Sci.* **1997**, *372*, 100.
- (20) Nishida, N.; Hara, M.; Sasabe, H.; Knoll, W. *Jpn. J. Appl. Phys.* **1997**, *36*, 2379.
- (21) Laibinis, P. E.; Whitesides, G. M.; Allara, D. L.; Tao, Y. T.; Parikh, A. N.; Nuzzo, R. G. *J. Am. Chem. Soc.* **1991**, *113*, 7152.
- (22) Fenter, P.; Eberhardt, A.; Eisenberger, P. *Science* **1994**, *266*, 1216.
- (23) Bryant, M. A.; Pemberton, J. E. *J. Am. Chem. Soc.* **1991**, *113*, 3630.
- (24) Leudtke, W. D.; Landman, U. *J. Phys. Chem.* **1996**, *100*, 13324.
- (25) Leudtke, W. D.; Landman, U. *J. Phys. Chem. B* **1998**, *102*, 6566.
- (26) Terrill, R. H.; Postlethwaite, T. A.; Chen, C.-H.; Poon, C.-D.; Terzis, A.; Chen, A.; Hutchinson, J. E.; Clark, M. R.; Wignall, G.; Londono, J. D.; Superfine, R.; Falvo, M.; Johnson, C. S., Jr.; Samulski, E. T.; Murray, R. W. *J. Am. Chem. Soc.* **1995**, *117*, 12537.